Theor Chem Acc (1998)
DOI 10.1007/s002149800m25

Theoretical
Chemistry Accounts

Regular article

Theoretical study of the valence $\pi \rightarrow \pi^*$ excited states of polyacenes: anthracene and naphthacene*

Yukio Kawashima, Tomohiro Hashimoto, Haruyuki Nakano, Kimihiko Hirao

Department of Applied Chemistry, Graduate School of Engineering, The University of Tokyo, Tokyo, 113-8656 Japan

Received: 22 April 1998 / Accepted: 6 July 1998 / Published online: 28 September 1998

Abstract. The valence $\pi \rightarrow \pi^*$ excited states of anthracene and naphthacene are studied with multireference perturbation theory with complete active space self-consistent field reference functions. The predicted spectra provide a consistent assignment of all one- and two-photon spectra and T-T spectra of low-lying valence $\pi \rightarrow \pi^*$ excited states of anthracene and naphthacene. The present theory predicts the valence $\pi \rightarrow \pi^*$ excitation energies with an accuracy of 0.15 eV for anthracene and of 0.25 eV or better for naphthacene. The excited states of anthracene and naphthacene are compared with those of benzene and naphthalene studied previously. The present calculations predict that, going from anthracene to naphthacene, there is a symmetry reversal of the two lowest singlet state transitions, but not for the triplet, just as indicated by the experimental data. Some general trends of polyacene excited states are discussed based on the calculated results for benzene to naphthacene. Conclusive results obtained for anthracene and naphthacene can be used as a model for understanding the excited states of larger polyacenes.

Key words: Multireference Møller-Plesset theory – Excited states of polyacenes – Anthracene – Naphthacene – Alternancy symmetry

1 Introduction

Since most polyacenes are far too large for rigorous *ab initio* treatment, a number of semiempirical methods have been used to obtain an approximate quantum mechanical description of large π-electron systems since the pioneering work of Pariser [1]. These methods seem to provide fairly good descriptions of the energy spectra, at least for the singly excited states, but fail to give equally good descriptions of the doubly excited states.

Recently, accurate ab initio quantum computational chemistry has evolved dramatically. The size of molecular systems which can be studied accurately using ab initio methods is increasing very rapidly. Especially, multireference based perturbation theory, such as CASPT2 the complete active space self-consistent field plus second-order perturbation theory (CASPT2) by Roos et al. [2] and our multireference Møller-Plesset theory (MRMP) [3], have opened a world of new possibilities. Real systems can be treated with predictive accuracy. Computational quantum chemistry is becoming an integral part of chemical research.

In a previous study, MRMP was applied to the study of the valence $\pi \rightarrow \pi^*$ excited states of polyenes [4] and benzene and naphthalene [5]. In addition to spin and spatial symmetries, the Hückel and Pariser-Parr-Pople (PPP) [6] model Hamiltonians for alternating hydrocarbons are known to yield the so-called alternancy symmetry [7] which classifies covalent minus (−) states and ionic plus (+) states. The attributes covalent and ionic stem from the character of the states in a valence bond description [8]. Covalent minus states and ionic plus states exhibit different behavior as far as electron correlation is concerned. Ionic plus states are dominated by single excitations, but covalent minus states include a large fraction of doubly excited configurations. Dynamic σ–π polarization effects are significant for ionic plus states, since π ionic configurations strongly polarize the σ space. These effects are taken into account by the second-order perturbation treatment in MRMP based on the complete active space self-consistent field (CASSCF) [9] reference function.

In the case of polyenes, the nature of the two lowest-lying singlet excited states, $1^1B_u^+$ and $2^1A_g^-$, and their ordering has been the most controversial issue [10]. The $1^1B_u^+$ state is a singly excited state with an ionic nature originating from a HOMO $\rightarrow$ LUMO one-electron transition, while the covalent $2^1A_g^-$ state is the doubly excited state which comes mainly from a (HOMO)^2 $\rightarrow$ (LUMO)^2 transition. MRMP predicts the two states to be virtually degenerate in hexatriene and after hexatriene, the doubly excited $2^1A_g^-$ state to be the lowest [4].

* Contribution to the Kenichi Fukui Memorial Issue

Correspondence to: K. Hirao

Contrary to the polyene case, the absorption and emission spectra of the polyacenes apparently do not show any anomalies. The absorption spectra mainly consist of three bands corresponding to $1^1B_{3u}^-$, $1^1B_{2u}^+$, and $1^1B_{3u}^+$ states in the notation of the D_{2h} group [11, 12]. In previous papers [5], the low-lying valence $\pi \rightarrow \pi^*$ excited states of benzene and naphthalene were studied with MRMP. The MRMP transition energies are in good agreement with experimental data. The valence excitation energies of benzene, for example, are predicted with an accuracy of 0.06 eV for singlet states and 0.14 eV or better for triplet states.

The purpose of the present paper is to study the excited states of polyacenes systematically. We report MRMP calculations for the excited states of anthracene and naphthacene. To our knowledge a sufficiently quantitative ab initio treatment for such large polyacenes has not been given so far. In Sect. 2 we summarize the computational details. MRMP excitation energies of anthracene and naphthacene are presented and discussed in Sect. 3. A comparative study of excited states from benzene to naphthacene is also given in Sect. 3.

2 Computational details

The calculations were carried out for the ground and low-lying singlet and triplet $\pi \rightarrow \pi^*$ excited states of anthracene and naphthacene. The ground state geometries of anthracene and naphthacene are optimized at the CASSCF and SCF levels, respectively, so the excitation energies calculated are vertical in nature. The molecules are placed in the xy plane with the long molecular axis corresponding to the x axis. Both molecules have D_{2h} symmetry. Thus, the dipole-allowed transitions of B_{3u} and B_{2u} are polarized along the long (x) and short (y) axes, respectively.

The basis sets used for carbon and hydrogen are Dunning's cc-pVDZ [13]. The onset of Rydberg excitation appears above 6 eV in anthracene. Thus, the Rydberg functions are not included in the present treatment. We examined the effect of the polarization functions of H numerically in a previous paper [5b] and found that polarization functions on H have little effect on the valence $\pi \rightarrow \pi^*$ excitation energies. Thus, we used Dunning's cc-pVDZ for carbon and hydrogen but without polarization on H.

We first carried out the state-averaged CASSCF calculations. The active space should include valence π and π^* orbitals in a balanced way in alternant hydrocarbons. For both molecules, 12 π electrons are treated as active electrons and distributed among 6 bonding π and 6 antibonding π^* orbitals. Perturbation calculations were performed with the MRMP method. The influence of the σ electrons and the remaining π electrons is included in a perturbation treatment. MRMP was applied to each individual state. The excitation energies calculated with respect to the ground state are all computed using the same method. Oscillator strengths were calculated using transition moments computed at the CASSCF level and with the MRMP transition energies.

3 Results and discussion

Figure 1 shows the geometries of anthracene and naphthacene optimized at the CASSCF and SCF level, respectively. Both molecules are completely planar with D_{2h} symmetry. Calculated bond lengths and bond angles for anthracene show good agreement with the experimental ones [14] listed in parentheses. We also calculated the geometry of anthracene at the SCF level. Although there are small changes between CASSCF and SCF data, the SCF geometry also agrees reasonably well with experiment. However, there is a considerable difference between the SCF geometry and the crystallographic data for naphthacene [15]. The maximum differences from the experimental results are 0.031 Å for the central bonds and 0.035 Å for the other bonds.

The polyacene occupied π orbitals are designated by 1,2,3,..., from the highest one down and the unoccupied orbitals by 1′,2′,3′,..., from the lowest one up. For anthracene, the occupied π orbitals 1,2,3,...,7 correspond to $2b_{3g}$, $2b_{2g}$, $1a_u$, $1b_{3g}$, $2b_{1u}$, $1b_{2g}$, and $1b_{1u}$, and the unoccupied ones 1′,2′,3′,...,7′ to $3b_{1u}$, $2a_u$, $3b_{2g}$, $4b_{1u}$, $3b_{3g}$, $3a_u$, and $4b_{3g}$, respectively. For naphthacene, 1,2,3,... correspond to $2a_u$, $3b_{1u}$, $2b_{3g}$, $1a_u$, $2b_{2g}$, $1b_{3g}$,...

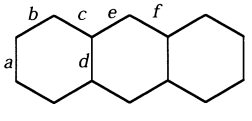

a = 1.420 (1.419)
b = 1.361 (1.366)
c = 1.438 (1.433)
d = 1.427 (1.436)
e = 1.397 (1.399)

$\angle ab$ = 120.6° (120.7°)
$\angle bc$ = 120.8° (120.6°)
$\angle ce$ = 122.1° (121.8°)
$\angle ef$ = 121.6° (121.0°)

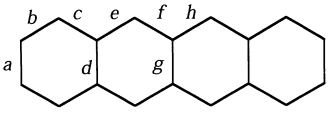

a = 1.444 (1.46)
b = 1.345 (1.38)
c = 1.446 (1.42)
d = 1.440 (1.42)
e = 1.376 (1.39)
f = 1.410 (1.40)
g = 1.429 (1.46)

$\angle ab$ = 120.6°
$\angle bc$ = 121.0°
$\angle cd$ = 118.4°
$\angle de$ = 119.5°
$\angle ef$ = 121.6°
$\angle fg$ = 118.9°

Fig. 1. The ground state geometry of anthracene optimized at the CASSCF level and that of naphthacene optimized at the Hartree-Fock level. The experimental values are given in parentheses. The C-C bond length is given in Å and the bond angle in degrees

and 1′, 2′, 3′,... to $3b_{2g}$, $3b_{3g}$, $4b_{1u}$, $4b_{2g}$, $3a_u$, $5b_{1u}$,..., respectively. The occupied orbital i and the unoccupied orbital i' are called a conjugated pair. For polyacenes, a conjugated pair (i, i') has a symmetry of (a_u, b_{2g}) or (b_{1u}, b_{3g}) in D_{2h} symmetry. The excited state considered in this calculation has either A_g, B_{1g}, B_{2u} or B_{3u} symmetry. Among these π orbitals, six highest occupied p orbitals and six lowest unoccupied π^* orbitals are employed as active orbitals in the reference CASSCF calculations.

The electric dipole transition moment vectors for the one-electron $i \rightarrow j'$ and $j \rightarrow i'$ ($i \neq j$) transitions are similar in magnitude and parallel in their orientation (for $i \rightarrow i'$ transitions the dipole transition moment vector for $1 \rightarrow 1'$ is antiparallel to that for $2 \rightarrow 2'$ and parallel to that for $3 \rightarrow 3'$). Thus, the dipole transition moment between any two plus states or between any two minus states is zero. That is, only transitions between plus and minus states are allowed (polyacenes have a center of symmetry which gives rise to the following selection rules: $u \rightarrow u$ and $g \rightarrow g$ transitions are always one-photon forbidden whereas $u \rightarrow g$ and $g \rightarrow u$ transitions are two-photon forbidden).

The HOMO $\rightarrow$ LUMO ($1 \rightarrow 1'$) excitation gives rise to the lowest $^1B_{2u}^+$ state with ionic nature. The two single excitations of $1 \rightarrow 2'$ and $2 \rightarrow 1'$ result in a pair of covalent $^1B_{3u}^-$ and ionic $^1B_{3u}^+$ states. Transitions to $^1B_{3u}^-$ are pseudoparity forbidden while transitions to $^1B_{2u}^+$ and $^1B_{3u}^+$ are dipole allowed. Transitions from 2 to 3′ with its alternancy symmetry conjugate of $3 \rightarrow 2'$ give dipole forbidden $^1A_g^-$ states. Double excitation of $(1)^2 \rightarrow (1')^2$ also gives rise to $^1A_g^-$, which lies in this energy range. If such a state exists it interacts with the singly excited $^1A_g^-$ states. Two single excitations of $1 \rightarrow 3'$ and $3 \rightarrow 1'$ give rise to a pair of covalent $^1B_{1g}^-$ and ionic $^1B_{1g}^+$ states. Similarly double excitations of $(1)^2 \rightarrow (1')(2')$ and its conjugate give $^1B_{1g}^-$ in this energy range. The double excitations are expected to have a profound effect on the description of the dipole-forbidden $^1A_g^-$ and $^1B_{1g}^-$ states of polyacenes.

In polyacene absorption spectra [11, 12], the lowest weak band is $^1B_{3u}^-$ and this has sharp vibrational structure with individual vibrational peaks about 300 cm^{-1} in half-width. The $^1B_{2u}^+$ band is of medium intensity and lies below all other strong and medium intensity transitions. It is short-axis polarized and characterized by a strong vibrational progression. For each additional aromatic ring in the molecule this transition is shifted 4000 to 8000 cm^{-1} to the red. The $^1B_{3u}^+$ band is the strongest. It is a long-axis polarized transition. The vibrational structure is even more diffuse, so often no clear minima can be seen. The second strongest is the $2^1B_{2u}^+$ band. It is broad and almost symmetrical and shows little structure.

For triplet excited states the HOMO $\rightarrow$ LUMO excitation gives rise to the lowest $^3B_{2u}^-$ state with a covalent nature. The two single excitations of $1 \rightarrow 2'$ and $2 \rightarrow 1'$ result in a pair of covalent $^3B_{3u}^-$ and ionic $^3B_{3u}^+$ states. Transitions from 2 to 3′ and its conjugate give the lowest $^3A_g^-$ state. In contrast to the corresponding singlet state, a double excitation of $(1)^2 \rightarrow (1')^2$ is prohibited from interacting with $^3A_g^-$ by spin symmetry. Two one-electron transitions of $1 \rightarrow 3'$ and $3 \rightarrow 1'$ give rise to a pair of covalent $^3B_{1g}^-$ and ionic $^3B_{1g}^+$ states. Double excitations of $(1)^2 \rightarrow (1')(2')$ will interact with the singly excited $^3B_{1g}^+$ state. Thus, most low-lying triplet states, except $1^3B_{1g}^+$, are expected to be dominated by the singly excited configurations.

The lowest triplet excited state in polyacenes is the 1^3B_{2u} state, which is well established by experiment [16]. Transitions from the lowest 1^3B_{2u} state to some of the higher ^3A_g and $^3B_{1g}$ levels are allowed. Thus, the major source of experimental information about the triplet states comes from the triplet-triplet (T-T) absorption spectrum. Experimental information about the higher $^3B_{3u}$ and $^3B_{2u}$ states is rather limited.

In the following sections we present and discuss the results calculated for anthracene and naphthacene separately and also compare the present data with previous semiempirical results and available experimental data. We also discuss the general trends of excited states of polyacenes from benzene to naphthacene.

3.1 Excited states of anthracene

The CASSCF configurations for the ground and low-lying valence $\pi \rightarrow \pi^*$ excited states are given in Table 1. The ground state is well described by the Hartree-Fock configuration. The ground state is of a covalent character. The energy is computed to be –537.77688 a.u. at the MRMP level. Vertical excitation energies and oscillator strengths calculated with the experimental data available are summarized in Table 2. Although previous ab initio calculations are limited in number, there are many semiempirical calculations [17–21] for the spectrum of anthracene following Pariser's work [1]. The present results are compared to the previous semiempirical calculations in Table 3.

3.1.1 Two lowest singlet excited states of anthracene

In the spectroscopic study of anthracene the search for the $1^1B_{3u}^-$ state near the $1^1B_{2u}^+$ band with onset at 3.27 eV seems to be the most controversial issue. The situation has been reviewed by Wolf and Hohlneicher [22]. Since the early work of Platt [23] and Clar [24], it has been assumed that the transition from the ground state to the lowest singlet B_{3u} state in anthracene is hidden under the medium-intense 1^1A_g, 1^1B_{2u} transition which starts at 27 695 cm^{-1} (3.43 eV) in the free molecule. All subsequent theoretical calculations have consistently shown that the origin of the two transitions should be close together but the reliability of the theoretical methods was not good enough to decide the location of the hidden B_{3u} state. A considerable amount of effort has been used to solve the problem experimentally. Since the two transitions are polarized perpendicularly to each other, spectroscopy with polarized light was thought to be a good choice. Along these lines, the identification of the long-axis polarized B_{3u} transition has been claimed several times with origins between 27 850 (3.45 eV) and 29 000 cm^{-1} (3.60 eV) [25–27]. However, all dichroism measurements suffer from the very low intensity of the B_{3u} transition.

Table 1. Main configurations in CASSCF(12,12) wavefunction of anthracene

State	Singlet transitions	Coefficients	State	Triplet transitions	Coefficients
$1^1A_g^-$					
$(7)^2(6)^2(5)^2(4)^2(3)^2(2)^2(1)^2$		0.8804			
$1^1B_{3u}^-$			$1^3B_{3u}^-$		
	$2 \rightarrow 1'$	0.6003		$2 \rightarrow 1'$	0.6112
	$1 \rightarrow 2'$	–0.5886		$1 \rightarrow 2'$	–0.5474
$1^1B_{2u}^+$			$1^3B_{2u}^-$		
	$1 \rightarrow 1'$	0.8753		$1 \rightarrow 1'$	0.8068
	$2 \rightarrow 2'$	0.1613		$2 \rightarrow 2'$	0.1761
$1^1B_{1g}^-$			$1^3B_{1g}^-$		
	$3 \rightarrow 1'$	0.5929		$3 \rightarrow 1'$	0.6053
	$1 \rightarrow 3'$	–0.3805		$1 \rightarrow 3'$	–0.5610
	$1,2 \rightarrow (1')^2$	0.3409			
	$(1)^2 \rightarrow 1',2'$	–0.2768			
$1^1B_{2u}^-$			$2^3B_{2u}^-$		
	$4 \rightarrow 1'$	0.5879		$4 \rightarrow 1'$	0.5572
	$1 \rightarrow 4'$	–0.4848		$1 \rightarrow 4'$	–0.5272
$1^1B_{3u}^+$			$1^3B_{3u}^+$		
	$2 \rightarrow 1'$	0.6091		$2 \rightarrow 1'$	0.5597
	$1 \rightarrow 2'$	0.6190		$1 \rightarrow 2'$	0.6424
$1^1B_{1g}^+$			$1^3B_{1g}^+$		
	$1 \rightarrow 3'$	0.6479		$1 \rightarrow 3'$	0.5522
	$3 \rightarrow 1'$	0.4967		$3 \rightarrow 1'$	0.5873
	$(1)^2 \rightarrow 1',2'$	0.2175		$(1)^2 \rightarrow 1',2'$	0.2326
	$1,2 \rightarrow (1')^2$	0.0735		$1,2 \rightarrow (1')^2$	0.1995
$2^1A_g^-$			$1^3A_g^-$		
	$(1)^2 \rightarrow (1')^2$	0.5304		$5 \rightarrow 1'$	0.4788
	$3 \rightarrow 2'$	–0.3517		$1 \rightarrow 5'$	–0.3732
	$2 \rightarrow 3'$	0.3258		$3 \rightarrow 2'$	–0.3996
	$5 \rightarrow 1'$	–0.2179		$2 \rightarrow 3'$	0.3990
	$1 \rightarrow 5'$	0.1655			
$2^1B_{3u}^-$					
	$3,1 \rightarrow (1')^2$	0.4305			
	$(1)^2 \rightarrow 1',3'$	–0.4023			
	$6 \rightarrow 1'$	0.2586			
	$1 \rightarrow 6'$	–0.1596			
	$3 \rightarrow 2'$	–0.2442			
	$2 \rightarrow 3'$	0.2240			
	$5 \rightarrow 3'$	0.2135			
	$3 \rightarrow 5'$	–0.1761			
$2^1B_{2u}^+$			$3^3B_{2u}^-$		
	$2 \rightarrow 2'$	0.8048		$2 \rightarrow 2'$	0.8046
	$3 \rightarrow 3'$	0.2038		$1 \rightarrow 1'$	0.1565
	$1 \rightarrow 1'$	–0.1012			

Up until now, the most conclusive estimates for the position of the 1^1B_{3u} transition come from two-photon absorption spectroscopy. In the early work of Bergman and Jortner [28], the low energy part of the two-photon excitation spectrum appeared to consist of two bands: a weak one around 28 000 cm^{-1} (3.47 eV) and a strong one around 31 000 cm^{-1} (3.84 eV). The 0–0 transitions of $^1B_{3u}$ and $^1B_{2u}$ are two-photon forbidden by symmetry since the final states are *u* states in both cases. According to the pseudoparity selection rules, 1^1B_{3u} should gain higher intensity than 1^1B_{2u} in two-photon absorption, exactly the reverse of the one-photon case. Another claim for the identification of the 1^1B_{3u} state at 27 800 cm^{-1} (3.45 eV) came from an MCD study of anthracene in cyclohexane [29]. More recent two-photon excitation spectra of anthracene [22] suggest that the onset of the hidden 1^1B_{3u} transition to the second excited singlet state lies at about 28 000 cm^{-1} (3.47 eV) in non-polar solvents. The correction for solvent shifts leads to an estimate of the separation between the origins of the two transitions in the free molecule of less than 500 cm^{-1} (0.062 eV).

MRMP predicts that the lowest singlet excited state is $^1B_{3u}^-$ and the second valence excited state is $^1B_{2u}^+$. The $^1B_{3u}^-$ state is calculated to lie at 3.23 eV while the $1^1B_{2u}^+$ state is predicted to appear at 3.40 eV. The MRMP excitation energy of 3.40 eV to $^1B_{2u}^+$ is very close to the observed peak at 3.43 eV in the absorption spectrum [30]. The $^1B_{3u}^-$ state is well described by the singly excited $\pi \rightarrow \pi^*$ transitions of $1 \rightarrow 2'$ and $2 \rightarrow 1'$, which have nearly the same weight but a different sign. The $^1B_{3u}^-$ state is a covalent minus state and the transition from the ground state is pseudoparity forbidden. The computed oscillator strength of 0.0004 for the transition to $^1B_{3u}^-$ is very low of 0.0004. On the other hand the ionic plus $1^1B_{2u}^+$ state comes mainly from the HOMO $\rightarrow$ LUMO ($1 \rightarrow 1'$) excitation but also contains the $2 \rightarrow 2'$ transition. The calculated oscillator strength is

0.083. Theory predicts that the $^1B^-_{3u}$ transition is at least two orders of magnitude weaker than the $1^1B^+_{2u}$ transition. This margin corresponds roughly to the intensity ratio calculated in naphthalene [5b] where $1^1B^-_{3u}$ lies at lower energy than $1^1B^+_{2u}$.

MRMP predicts $1^1B^-_{3u}$ 0.17 eV below $1^1B^+_{2u}$ in anthracene, in disagreement with the assignment of a two-photon absorption [22, 28]. Our experience suggests that MRMP tends to underestimate the lowest covalent state by about 0.1–0.2 eV. If this is the case, the $1^1A^-_g \rightarrow 1^1B^-_{3u}$ transition is located in the immediate vicinity of the $1^1A^-_g \rightarrow 1^1B^+_{2u}$ excitation. The location of the hidden $1^1B^-_{3u}$ state relative to the optically allowed $1^1B^+_{2u}$ state is still an open question.

Table 2. Calculated valence singlet excitation energies (eV) of anthracene[a]

State	CASSCF	MRMP	Experiment
$1^1B^-_{3u}$	4.57	3.23 (0.0004)	3.84[b], 3.45[c]
$1^1B^-_{2u}$	5.29	3.40 (0.0827)	3.31 (0.1)[d], 3.43[e]
$1^1B^-_{1g}$	6.07	4.30	4.12[b], 4.44[f]
$1^1B^-_{2u}$	7.18	4.32 (0.0012)	
$1^1B^+_{1g}$	7.06	4.63	4.66[b], 4.83[f]
$1^1B^+_{3u}$	7.44	4.77 (1.9377)	4.84 (2.28)[d], 4.92[g], 5.24[h]
$2^1A^-_g$	5.42	5.03	4.96[b], 4.71[f]
$3^1A^-_g$	6.57	5.28	5.33[f]
$2^1B^-_{3u}$	7.44	5.33 (0.0026)	
$2^1B^+_{2u}$	7.70	5.67 (0.1436)	5.61 (0.28)[d], 5.80 (0.23)[h]

[a] The oscillator strengths are given in parentheses
[b] Bergman A, Jortner J (1972) Chem Phys Lett 15: 309
[c] Steiner RP, Michl J (1978) J Am Chem Soc 100: 6861
[d] Klevens HB, Platt JR (1949) J Chem Phys 17: 470
[e] Lambert WR, Felker PM, Syage JA, Zewail AH (1984) J Chem Phys 81: 2195
[f] Dick B, Hohlneicher G (1981) Chem Phys Lett 83: 615
[g] Suzuki H (1967) Electronic Absorption Spectra and Geometry of Organic Molecules, Academic, New York
[h] Lyons LE, Morris GC (1960) J Mol Spectrosc 4: 480

3.1.2 Higher $\pi \rightarrow \pi^*$ singlet excited states of anthracene

The two-photon absorbic spectrum of anthracene measured in solution shows a broad band with a maximum at 4.12–4.44 eV [28, 31]. This peak is assigned to $1^1B^-_{1g}$ from the analysis of the two-photon polarization. Theory predicts the third valence excited state to be $1^1B^-_{1g}$. This state comes mainly from the single excitations of $1 \rightarrow 3'$ and $3 \rightarrow 1'$ but includes a large fraction of doubly excited configurations of $(\text{HOMO})^2 \rightarrow (\text{LUMO})(\text{LUMO}+1)$ and its conjugate. The $1^1B^-_{1g}$ is a covalent state and has a character of a multireference nature. MRMP predicts this state to lie at 4.30 eV, in agreement with the observed peak of 4.44 eV in the two-photon spectrum in ethanol solution [31]. The excitation energy observed from the two-photon spectrum in benzene solution is 4.12 eV [28]: this is quite low

Table 3. Comparison of MRMP excitation energies (eV) of anthracene singlet states with semi-empirical results[a]

State	MRMP	Experiment	Pariser[i]	SCF-RPA[j]	exact PPP[k]	PPP-SCF[l]	CNDO/S[d]	CNDO/S2[m]
$1^1B^-_{3u}$	3.23 (0.0004)	3.84[b], 3.45[c]	3.72	3.66	3.23	3.59	3.78 (0.0014)	3.74
$1^1B^+_{2u}$	3.40 (0.0827)	3.31 (0.1)[d] 3.43[e]	3.65 (0.386)	3.84 (0.12)	3.68	3.49 (0.312)	3.68 (0.1173)	3.36
$1^1B^-_{1g}$	4.30	4.12[b], 4.44[f]	4.61	4.80	4.31	4.62	4.79	4.57
$1^1B^-_{2u}$	4.32 (0.0012)		5.69		4.97	5.27	5.28	
$1^1B^+_{1g}$	4.63	4.66[b], 4.83[f]	4.94	5.81	4.81	4.68	5.17	4.80
$1^1B^+_{3u}$	4.77 (1.9377)	4.84 (2.28)[d], 4.92[g], 5.24[h]	5.50 (3.229)	5.71 (2.47)	5.36 (0.1935)	4.83 (2.52)	5.62 (2.251)	4.95
$2^1A^-_g$	5.03	4.96[b], 4.71[f]	5.00	5.30	3.88	4.82	4.96	5.21
$3^1A^-_g$	5.28	5.33[f]	6.82	6.74	4.96	6.06	5.63	6.72
$2^1B^-_{3u}$	5.33 (0.0026)		6.24	6.74	4.88		6.05 (0.0011)	
$2^1B^+_{2u}$	5.67 (0.1436)	5.61 (0.28)[d], 5.80 (0.23)[h]	5.25 (0.091)	5.52 (0.13)	5.71 (0.005)	5.72 (0.186)	5.77 (0.1081)	5.53

[a] The oscillator strengths are given in parentheses
[b] Bergman A, Jortner J (1972) Chem Phys Lett 15: 309
[c] Steiner RP, Michl J (1978) J Am Chem Soc 100: 6861
[d] Klevens HB, Platt JR (1949) J Chem Phys 17: 470
[e] Lambert WR, Felker PM, Syage JA, Zewail AH (1984) J Chem Phys 81: 2195
[f] Dick B, Hohlneicher G (1981) Chem Phys Lett 83: 615
[g] Suzuki H (1967) Electronic Absorption Spectra and Geometry of Organic Molecules, Academic, New York
[h] Lyons LE, Morris GC (1960) J Mol Spectrosc 4: 480
[i] Pariser R (1956) J Chem Phys 24: 250
[j] Baldo M, Grassi A, Pucci R, Tomasello P (1982) J Chem Phys 77: 2438
[k] Ramesesha S, Galvao DS, Soos ZG (1993) J Phys Chem 97: 2823
[l] Alderich DM, Mathies R, Albrecht AC (1974) J Mol Spectrosc 51: 166
[m] Lipari NO, Duke CB (1975) J Chem Phys 63: 1768

compared to the other results. The exact PPP method [19] computes the excitation to be 4.31 eV, which is close to our value: however, other semiempirical calculations yield, not surprisingly, an excitation energy about 0.3 eV larger than calculated by MRMP.

The fourth state is computed to be $1^1B_{2u}^-$. This state mainly consists of configurations of $1 \rightarrow 4'$ and its conjugate. The transition is pseudoparity forbidden. The computed excitation energy is 4.32 eV with an oscillator strength of 0.0012. Margulies and Yogev [32] observed a very weak short-axis polarized absorption at 4.68 eV. This band is partially hidden by the strong $1^1B_{3u}^+$ band and might be attributed to $1^1B_{2u}^-$. The calculated weak intensity confirms that the $1^1B_{2u}^-$ band must be partially hidden behind the intense $1^1B_{3u}^+$ band. Other calculations locate this state above 5.0 eV.

The two-photon absorption spectrum in benzene solution shows a peak at 4.66 eV [28]. MRMP predicts that this is due to the $1^1A_g^- \rightarrow 1^1B_{1g}^+$ transition. The main configurations are $3 \rightarrow 1'$ and $1 \rightarrow 3'$ but they mix with the same sign. MRMP calculates the excitation energy to be 4.63 eV, which shows good agreement with the experimental result measured in benzene solution. The two-photon absorption spectrum in ethanol shows this state at 4.83 eV [31]. The CNDO/S [12] and SCF-RPA [18] calculations yield considerably larger excitation energies of 5.17 and 5.81 eV, respectively.

The strongest band in the absorption spectrum of anthracene appears at about 5 eV. This band is due to the $1^1A_g^- \rightarrow 1^1B_{3u}^+$ transition and is well characterized experimentally. The absorption spectrum in *n*-heptane solution shows the $1^1B_{3u}^+$ state at 4.84 eV with an oscillator strength of 2.28 [12] and in the gas-phase absorption spectrum it is at 4.92 eV [33]. The $1^1B_{3u}^+$ state is well described by the one-electron transitions of $1 \rightarrow 2'$ and its conjugate. MRMP predicts that $1^1B_{3u}^+$ appears at 4.77 eV. The calculated oscillator strength of 1.938 is consistent with the fact that this is the most intense transition in the spectrum. Semiempirical methods estimate the vertical excitation energy for $1^1B_{3u}^+$ to be in the range 4.83–5.71 eV.

The next two states are the dipole-forbidden $2^1A_g^-$ and $3^1A_g^-$ states. Both come mainly from doubly excited $(\text{HOMO})^2 \rightarrow (\text{LUMO})^2$, and singly excited $3 \rightarrow 2'$ and $2 \rightarrow 3'$ transitions. The strong admixture of the double excitation to the wavefunction of $2^1A_g^-$ had been noted previously by Michl et al [34]. MRMP computes the excitation energies of $2^1A_g^-$ and $3^1A_g^-$ to be 5.03 eV and 5.28 eV, respectively. The former is close to the experimental value of 4.96 eV, measured in the two-photon absorption spectrum in benzene solution [28]. This peak was also found at 4.71 eV in the two-photon spectrum in ethanol solution [31]. The 5.28 eV excitation energy of 3^1A_g corresponds to the peak observed at 5.33 eV in the two-photon absorption study in ethanol solution [31].

Klevens and Platt [12] observed a band at 5.61 eV with an oscillator strength of 0.28 to the blue of the $1^1B_{3u}^+$ state of anthracene. Lyons and Morris [35] also observed a peak at 5.80 eV with an oscillator strength of 0.23. The polarization study reveals that the band is short-axis polarized [32]. Hence we assign the band to $2^1B_{2u}^+$ which is predicted to lie at 5.67 eV with an oscillator strength of 0.144. The state is well described by singly excited configurations of $2 \rightarrow 1'$ and its conjugate.

Between the $3^1A_g^-$ and $1^1B_{3u}^+$ states MRMP predicts the existence of the doubly excited $2^1B_{3u}^-$ state at 5.33 eV. The exact PPP method [19] locates this state at 4.88 eV but other calculations place the state above 6 eV.

3.1.3 Triplet $\pi \rightarrow \pi^*$ excited states of anthracene

The main configurations of the CASSCF wavefunctions for triplet excited states are given in Table 1. Calculated T-T excitation energies are listed in Table 4 and compared with other calculations in Table 5.

The lowest triplet state is $1^3B_{2u}^-$ due to the transition of $1 \rightarrow 1'$. MRMP predicts that the excitation energy of $1^1A_g^-$ ($S_0 \rightarrow T_1$) is 2.00 eV. The anthracene $S_0 \rightarrow T_1$ transition energy has recently been determined to be 1.869 eV from a photodetachment photoelectron spectroscopic study in the gas phase [36]. The discrepancy between theory and experiment is 0.131 eV.

The first triplet state above $1^3B_{2u}^-$ is computed to be $1^3B_{3u}^-$. This state mainly comes from transitions of $2 \rightarrow 1'$ and its conjugate. MRMP locates this state 1.30 eV above $1^3B_{2u}^-$. Pariser [1] predicts that this state lies at 1.84 eV, and PPP [16] at 1.85 eV, nearly 0.5 eV higher than MRMP. The excitation from $1^3B_{2u}^-$ to $1^3B_{2u}^-$ is dipole-forbidden and no experimental value has been reported.

The lowest dipole-allowed triplet state from $1^3B_{2u}^-$ is observed at 1.40 eV with an oscillator strength of 0.002 in the T-T absorption spectra in alcoholic solution [16]. The state is $1^3B_{1g}^-$. The calculated excitation energy is 1.35 eV and the oscillator strength is 0.0003, in fair agreement with experiment. The state mainly comes from transitions of $3 \rightarrow 1'$ and its conjugate. Meyer et al. [16] place $1^3B_{1g}^-$ at 1.49 eV while Pariser [1] places is at 1.18 eV. The four states following $1^3B_{1g}^-$ are computed to be dipole-forbidden *u* states. They are singly excited $1^3B_{3u}^-$, $1^3B_{2u}^+$, $1^3B_{3u}^+$, and $2^3B_{2u}^-$ states.

Table 4. Triplet-triplet excitation energies (eV) of anthracene[a]

States	CASSCF	MRMP	Experiment
Singlet–triplet energy gap (eV)			
$1^1A_g^- \rightarrow 1^3B_{2u}^-$	2.60	2.00	1.869[b]
Triplet–triplet transition energies (eV)			
$1^3B_{3u}^-$	1.67	1.30	
$1^3B_{1g}^-$	1.09	1.35 (0.0003)	1.40 (0.002)[c]
$1^3B_{2u}^+$	2.31	1.66	
$1^3B_{3u}^+$	3.01	2.02	
$2^3B_{2u}^-$	2.67	2.10	
$1^3A_g^-$	2.51	2.62 (0.0012)	2.40 (0.04)[c], 2.65[d]
$1^3B_{1g}^+$	4.40	2.74 (0.2192)	2.92 (0.25)[c], 2.92[d]
$1^3A_g^+$	5.11	3.03 (0.0002)	

[a] The oscillator strengths are given in parentheses
[b] Schiedt J, Weinkauf R (1997) Chem Phys Lett 266: 201
[c] Meyer YH, Astier R, Leclercq JM (1972) J Chem Phys 56: 801
[d] Porter G, Windsor MW (1958)
Proc Roy Soc (London) A245: 235

Table 5. Comparison of MRMP T-T excitation energies (eV) of anthracene with semi-empirical results[a]

States	MRMP	Experiment	Pariser[e]	PPP[c]	CNDO/S2[f]	SCF-RPA[g]
Singlet–triplet energy gap (eV)						
$1^1A_g^- \rightarrow 1^3B_{2u}^-$	2.00	1.869[b]	1.66		1.45	1.06
Triplet–triplet transition energies (eV)						
$1^3B_{3u}^-$	1.30	1.84	1.85	1.99		
$1^3B_{1g}^-$	1.35 (0.0003)	1.40 (0.002)[c]	1.18	1.49	1.42	2.01
$2^3B_{2u}^-$	1.66		1.90	2.26	3.10	
$1^3B_{3u}^+$	2.02		2.06	2.45	2.29	
$3^3B_{2u}^-$	2.10		3.57	3.67	4.11	
$1^3A_g^-$	2.62 (0.0012)	2.40 (0.04)[c], 2.65[d]	2.32	2.65	4.60	3.47
$1^3B_{1g}^+$	2.74 (0.2192)	2.92 (0.25)[c], 2.92[d]	3.28 (0.540)	3.14 (0.38)	3.35	4.65
$1^3A_g^+$	3.03 (0.0002)		3.32 (0.166)	3.80 (0.12)	4.16	4.24

[a] The oscillator strengths are given in parentheses
[b] Schiedt J, Weinkauf R (1997) Chem Phys Lett 266: 201
[c] Meyer YH, Astier R, Leclercq JM (1972) J Chem Phys 56: 801
[d] Porter G and Windsor MW (1958) Proc Roy Soc (London) A245: 235
[e] Pariser R (1956) J Chem Phys 24: 250
[f] Lipari NO, Duke CB (1975) J Chem Phys 63: 1768
[g] Baldo M, Grassi A, Pucci R, Tomasello P (1982) J Chem Phys 77: 2438

The second dipole-allowed state from the lowest triplet state is the pseudoparity forbidden $1^3A_g^-$ state. The wavefunction consists of singly excited configurations. MRMP predicts $1^3A_g^-$ at 2.62 eV with an oscillator strength of 0.001. It occurs at 2.65 eV [37] and 2.40 eV (with an oscillator strength of 0.04) [16] in the absorption spectra in dilute solution and alcohol solution, respectively. The PPP method [16] predicts the absorption peak to be at 2.65 eV, close to MRMP. The computed T-T excitation energy calculated with CNDO/S2 [21] is 4.60 eV, and SCF-RPA [18] gives 3.47 eV.

The most intense triplet state is the $1^3B_{1g}^+$ state. It is observed at 2.92 eV with an oscillator strength of 0.25 in the absorption spectrum in alcohol solution [16, 37]. MRMP computes $1^3B_{1g}^+$ to lie at 2.74 eV with an oscillator strength of 0.219, close to the experimental data. A large fraction of the CASSCF wavefunction for $1^3B_{1g}^+$ can be described as doubly excited with respect to the ground state. Thus, the $1^3B_{1g}^+$ state has a character of doubly excited nature. The $1^3B_{1g}^+$ state is the only state calculated as doubly excited among the low-lying triplet states treated here. The SCF-RPA method [18] places $1^3B_{1g}^+$ by 1 eV higher than MRMP and experimental results.

3.2 Excited states of naphthacene

Among 18 valence π orbitals in naphthacene, 12 π orbitals discarding the three lowest occupied ($1b_{1u}$, $1b_{2g}$, and $2b_{1u}$) and three highest unoccupied ($4b_{3g}$, $4a_u$, and $5b_{3g}$) orbitals, are employed as active orbitals in the reference CASSCF calculations. The CASSCF configurations for the ground and low-lying valence $\pi \rightarrow \pi^*$ excited states are given in Table 6. The ground state is again well-described by the Hartree-Fock configuration. The energy is computed to be −690.922469 a.u. at the MRMP level.

3.2.1 Singlet $\pi \rightarrow \pi^*$ excited states of naphthacene

Five singlet states are discernible in the absorption spectrum [38] of naphthacene ranging from 2.5 to 6.2 eV: S_1 (2.62, 2.72 eV), S_2 (4.22 eV), S_3 (4.50 eV), S_5 (5.39 eV) and S_6 (5.86 eV). The absorption polarization spectrum obtained by Zimmermann and Joop [39] indicates the existence of yet another state, S_4 (4.77 eV). In agreement with the polarization behavior observed by Zimmermann and Joop, Pariser [1] had assigned S_1 to the short-axis polarized $1^1B_{2u}^+$ state and S_3 to the long-axis polarized $1^1B_{3u}^+$ state. Pariser attributed S_2 to $2^1B_{2u}^+$, which is predicted below $1^1B_{3u}^+$ by an SCI calculation. However, Zimmermann and Joop [39] assigned the degree of polarization of the $S_1 \rightarrow S_0$ fluorescence to be constant and negative throughout the S_2 and S_3 bands. This implies that the $S_0 \rightarrow S_2$ transition must be long-axis polarized, in contrast to Pariser's assignment.

The calculated data for the excited singlet states of naphthacene are summarized in Tables 7 and 8. The HOMO → LUMO excitation gives rise to the lowest $1^1B_{2u}^+$ of an ionic nature. The MRMP excitation energy is 2.80 eV, in good agreement with the experimental value of 2.72 eV observed in the absorption spectrum in the gas phase [40]. The absorption spectrum of naphthacene in benzene solution shows a peak at 2.60 eV [41]. The calculated oscillator strength is 0.104, again in good agreement with the experimental value of 0.11. INDO/S calculates the transition energy to be 2.70 eV and the oscillator strength to be 0.282 [42].

The second excited state is the covalent $1^1B_{3u}^-$ state. The state is computed to lie 2.92 eV above the ground state. This must correspond to the peak at 3.12 eV found in the gas-phase absorption spectrum [40]. The state

Table 6. Main configurations in CASSCF(12,12) wavefunction of naphthacene

State	Singlet transitions	Coefficients	State	Triplet transitions	Coefficients
$1^1A_g^-$					
$\ldots(6)^2\ (5)^2(4)^2\ (3)^2(2)^2\ (1)^2$		0.8909			
$1^1B_{2u}^+$			$1^3B_{2u}^-$		
	$1 \rightarrow 1'$	0.8934		$1 \rightarrow 1'$	0.8549
				$3 \rightarrow 3'$	0.2122
$1^1B_{3u}^-$			$1^3B_{3u}^-$		
	$2 \rightarrow 2'$	0.6234		$2 \rightarrow 1'$	0.6136
	$1 \rightarrow 1'$	−0.5856		$1 \rightarrow 2'$	−0.5769
$1^1B_{1g}^-$			$1^3B_{1g}^-$		
	$3 \rightarrow 1'$	0.6234		$3 \rightarrow 1'$	0.6305
	$1 \rightarrow 3'$	−0.4364		$1 \rightarrow 3'$	−0.5560
	$1,2 \rightarrow (1')^2$	0.2793			
	$(1)^2 \rightarrow 1', 2'$	−0.2454			
$1^1B_{2u}^-$			$2^3B_{2u}^-$		
	$4 \rightarrow 1'$	0.5930		$4 \rightarrow 1'$	0.5247
	$1 \rightarrow 4'$	−0.4507		$1 \rightarrow 4'$	−0.5272
$1^1B_{3u}^+$			$1^3B_{3u}^+$		
	$2 \rightarrow 1'$	0.6400		$2 \rightarrow 1'$	0.6304
	$1 \rightarrow 2'$	0.5950		$1 \rightarrow 2'$	0.6671
$1^1B_{1g}^+$			$1^3B_{1g}^+$		
	$1 \rightarrow 3'$	0.6930		$1 \rightarrow 3'$	0.6318
	$3 \rightarrow 1'$	0.5345		$3 \rightarrow 1'$	0.5792
				$(1)^2 \rightarrow 1', 2'$	0.2066
				$1,2 \rightarrow (1')^2$	0.1769
$2^1B_{2u}^+$					
	$4 \rightarrow 1'$	0.5502			
	$1 \rightarrow 4'$	0.4504			
	$3 \rightarrow 3'$	−0.4721			
	$2 \rightarrow 2'$	−0.2050			
$2^1A_g^-$			$1^3A_g^-$		
	$(1)^2 \rightarrow (1')^2$	0.7080		$5 \rightarrow 1'$	0.5492
	$5 \rightarrow 1'$	0.2592		$1 \rightarrow 5'$	−0.3912
	$1 \rightarrow 5'$	−0.2026		$3 \rightarrow 2'$	0.3059
				$2 \rightarrow 3'$	−0.3013
$3^1B_{2u}^+$			3^3B_{2u}		
	$2 \rightarrow 2'$	0.5798		$2 \rightarrow 2'$	0.8046
	$3 \rightarrow 3'$	0.3990		$5 \rightarrow 5'$	0.2207
	$1 \rightarrow 4'$	0.3106			
	$4 \rightarrow 1'$	0.3552			
$2^1B_{3u}^-$					
	$3,1 \rightarrow (1')^2$	0.4731			
	$(1)^2 \rightarrow 1', 3'$	−0.4340			
$4^1B_{2u}^+$					
	$2 \rightarrow 2'$	0.5730			
	$3 \rightarrow 3'$	−0.5254			
	$(1)^2 \rightarrow 2', 3'$	−0.2186			
	$2,3 \rightarrow (1')^2$	0.0315			

comes from the transitions of $1 \rightarrow 2'$ and $2 \rightarrow 1'$. Thus, both theory and experiment confirm the inversion between $1^1B_{3u}^-$ and $1^1B_{2u}^+$ states in naphthacene.

MRMP predicts that there are three dipole-forbidden g states in the range 3.55–3.86 eV. These are a pair of covalent $1^1B_{1g}^-$ and ionic $1^1B_g^+$ states and the second $2^1A_g^-$ state. Note that the wavefunction of $2^1A_g^-$ is dominated by a doubly excited configuration of $(\text{HOMO})^2 \rightarrow (\text{LUMO})^2$.

The $S_0 \rightarrow S_2$ transition observed at 4.22 eV [41] is suggested to be long-axis polarized [39] in contrast to Pariser's assignment. Thus, S_2 must be $2^1B_{3u}^-$. MRMP locates $2^1B_{3u}^-$ at 4.24 eV, which is in good agreement with the observed peak. The computed oscillator strength is 0.012 while the observed one is 0.10. This state is described by $1,3 \rightarrow (1')^2$ and its conjugate. Since $2^1B_{3u}^-$ is described as doubly excited, previous calculations placed it at above 5 eV.

The most intense band (S_3) of the absorption spectrum of naphthacene in benzene solution appears at 4.50 eV with an oscillator strength of 1.75 [41]. This corresponds to the long-axis polarized $1^1B_{3u}^+$ state. The $1^1B_{3u}^+$ state is dominated by the singly excited configurations of $1 \rightarrow 2'$ and $2 \rightarrow 1'$. The state is predicted to lie at 4.32 eV with MRMP. The oscillator strength is computed to be 2.357.

MRMP predicts another state exists slightly below the intense $1^1B_{3u}^+$ band. The $1^1B_{2u}^-$ state is computed to exist at 4.28 eV with weak intensity. The state is pseudoparity forbidden. Thus, the transition from the ground state to $1^1B_{2u}^-$ must be hidden under the intense $1^1A_g \rightarrow 1^1B_{3u}^+$ transition.

The $1 \rightarrow 4'$ and $4 \rightarrow 1'$ transitions give rise to the ionic plus state of $2^1B_{2u}^+$. MRMP predicts that $2^1B_{2u}^+$ appears at 4.62 eV with medium intensity. Following the observations by Zimmermann and Joop [39] we assigned S_4 (4.77 eV) to $2^1B_{2u}^+$.

The absorption spectrum in benzene solution gives a peak at 5.39 eV with an oscillator strength of 0.28 [41]. This second most intense band (S_5) is assigned to $4^1B_{2u}^+$. MRMP calculates the excitation energy to be 5.63 eV and the oscillator strength to be 0.352. The state is described by a mixture of singly and doubly excited configurations.

Table 7. Calculated valence singlet $\pi \rightarrow \pi^*$ excitation energy (ev) of naphthacene[a]

State	CASSCF	MRMP	Experiment
$1^1B_{2u}^+$	4.47	2.80 (0.1039)	2.60[b] (0.11).2.72[c]
$1^1B_{3u}^-$	4.44	2.92 (0.0021)	3.12[c]
$1^1B_{1g}^-$	5.56	3.55	
$2^1A_g^-$	4.75	3.66	
$1^1B_{1g}^+$	5.99	3.86	
$2^1B_{3u}^-$	6.48	4.24 (0.0119)	4.22[b] (0.10)
$1^1B_{2u}^-$	6.26	4.28 (0.0011)	
$1^1B_{3u}^+$	6.94	4.32 (2.3567)	4.50[b] (1.75)
$2^1B_{2u}^+$	7.27	4.62 (0.0133)	
$3^1A_g^-$	6.37	4.66	
$3^1B_{2u}^+$	7.85	5.16 (0.0002)	
$4^1B_{2u}^+$	8.57	5.63 (0.3523)	5.39[b] (0.28)

[a] The oscillator strengths are given in parentheses
[b] Ref. [41]
[c] Ref. [40]

The dipole-forbidden $3^1A_g^-$ state and the very weak dipole-allowed $3^1B_{2u}^+$ state are predicted to exist between the S_4 and S_5 bands.

3.2.2 Triplet $\pi \rightarrow \pi^*$ excited states of naphthacene

Calculated T-T spectra of naphthacene are summarized in Tables 9 and 10. The lowest triplet excited state is $1^3B_{2u}^-$, which is well established by experiment. The state

Table 9. Triplet-triplet excitation energies (eV) of naphthacene[a]

States	CASSCF	MRMP	Experiment
Singlet–triplet energy gap (eV)			
$1^1A_g^- \rightarrow 1^3B_{2u}^-$	2.05	1.51	1.25[b], 1.30[c], 1.27[d]
Triplet–triplet transition energies (eV)			
$1^3B_{1g}^-$	1.46	0.92 (0.0002)	1.29[e]
$1^3B_{3u}^-$	2.30	1.45	
$2^3B_{2u}^-$	2.42	1.76	
$1^3B_{3u}^+$	3.45	2.01	
$1^3B_{1g}^+$	4.04	2.51 (0.4089)	2.68[e], 2.69[f], 2.55[g]
$3^3B_{2u}^-$	3.59	2.66	
$1^3A_g^-$	4.56	2.93 (0.0014)	2.58[e], 2.60[f], 3.01 [g]
$1^3A_g^+$	4.97	3.26 (0.0067)	3.66[e]
$2^3A_g^-$	3.58	4.34 (0.0024)	4.34[f], 4.34[g]

[a] The oscillator strengths are given in parentheses
[b] Tomkiewicz Y, Groff RP, Avakian P (1971) J Chem Phys 54: 4504
[c] Sabbatini N, Indelli MT, Gandolfi MT, Balzani V (1982) J Phys Chem 86: 3585
[d] McGlynn SP, Azumi T, Kasha M (1964) J Chem Phys 51: 507
[e] Meyer YH, Astier R, Leclercq JM (1972) J Chem Phys 56: 801
[f] Porter G, Windsor MW (1958) Proc Roy Soc London A245: 235
[g] Pavlopoulos TG (1972) J Chem Phys 56: 227

Table 8. Comparison of MRMP excitation energies (eV) of naphthacene singlet states with semi-empirical results[a]

State	MRMP	Experiment	Pariser[d]	INDO/S[e]	CNDO/S2[f]	SCF-RPA[g]
$^1B_{2u}^+$	2.80 (0.1039)	2.60[b](0.11), 2.72[c]	3.11 (0.442)	2.70 (0.2817)	2.77	3.35 (0.19)
$1^1B_{3u}^-$	2.92 (0.0021)	3.12[c]	3.57	3.19 (0.0733)	3.56	3.41
$1^1B_{1g}^-$	3.55		3.90	3.68	3.84	3.78
$2^1A_g^-$	3.66		4.51	4.27	5.21	4.73
$1^1B_{1g}^+$	3.86		4.26	3.96	3.99	4.51
$2^1B_{3u}^-$	4.24 (0.0119)	4.22[b] (0.10)	5.78	5.38 (0.00482)		5.99
$1^1B_{2u}^-$	4.28 (0.0011)		5.14	4.46 (0.0128)		
$1^1B_{3u}^+$	4.32 (2.3567)	4.50[b] (1.75)	5.09 (3.780)	4.49 (3.2899)	4.54	5.29 (3.25)
$2^1B_{2u}^+$	4.62 (0.0133)	4.77		5.08 (0.0488)		
$3^1A_g^-$	4.66		6.31	5.48		6.77
$3^1B_{2u}^+$	5.16 (0.0002)					
$4^1B_{2u}^+$	5.63 (0.3523)	5.39 [b] (0.28)	4.69 (0.159)			4.65 (0.11)

[a] The oscillator strengths are given in parentheses
[b] Ref. [41]
[c] Ref. [40]
[d] Ref. [1]
[e] Ref. [42]
[f] Ref. [21]
[g] Ref. [18]

Table 10. Comparison of MRMP T-T excitation energies (eV) of naphthacene with the semi-empirical results[a]

States	MRMP	Experiment	PPP[h]	CNDO/S2[i]	PPP[e]
Singlet–triplet energy gap (eV)					
$1^1A_g^- \rightarrow 1^3B_{2u}^-$	1.51	1.25[b], 1.30[c], 1.27[d]	1.10	0.98	
Triplet–triplet transition energies (eV)					
$1^3B_{1g}^-$	0.92 (0.0002)	1.29[e]	0.76	1.24	1.39
$1^3B_{3u}^-$	1.45		2.46	2.38	2.31
$2^3B_{2u}^-$	1.76		2.09		2.42
$1^3B_{3u}^+$	2.01		3.35	2.59	2.79
$1^3B_{1g}^+$	2.51 (0.4089)	2.68[e], 2.55[f], 2.69[g]	3.16 (1.304)	2.97	2.93
$3^3B_{2u}^-$	2.66				3.97
$1^3A_g^-$	2.93 (0.0014)	2.58[e], 3.01[f], 2.60[g]	2.65		2.44
$1^3A_g^+$	3.26 (0.0067)	3.66[e]			3.82

[a] The oscillator strengths are given in parentheses
[b] Tomkiewicz Y, Groff RP, Avakian P (1971) J Chem Phys 54: 4504
[c] Sabbatini N, Indelli MT, Gandolfi MT, Balzani V (1982) J Phys Chem 86: 3585
[d] McGlynn SP, Azumi T, Kasha M (1964) J Chem Phys 51: 507
[e] Meyer YH, Astier R, Leclercq JM (1972) J Chem Phys 56: 801
[f] Porter G, Windsor MW (1958) Proc Roy Soc London A245: 235
[g] Pavlopoulos TG (1972) J Chem Phys 56: 227
[h] Pariser R (1956) J Chem Phys 24: 250
[i] Lipari NO, Duke CB (1975) J Chem Phys 63: 1768

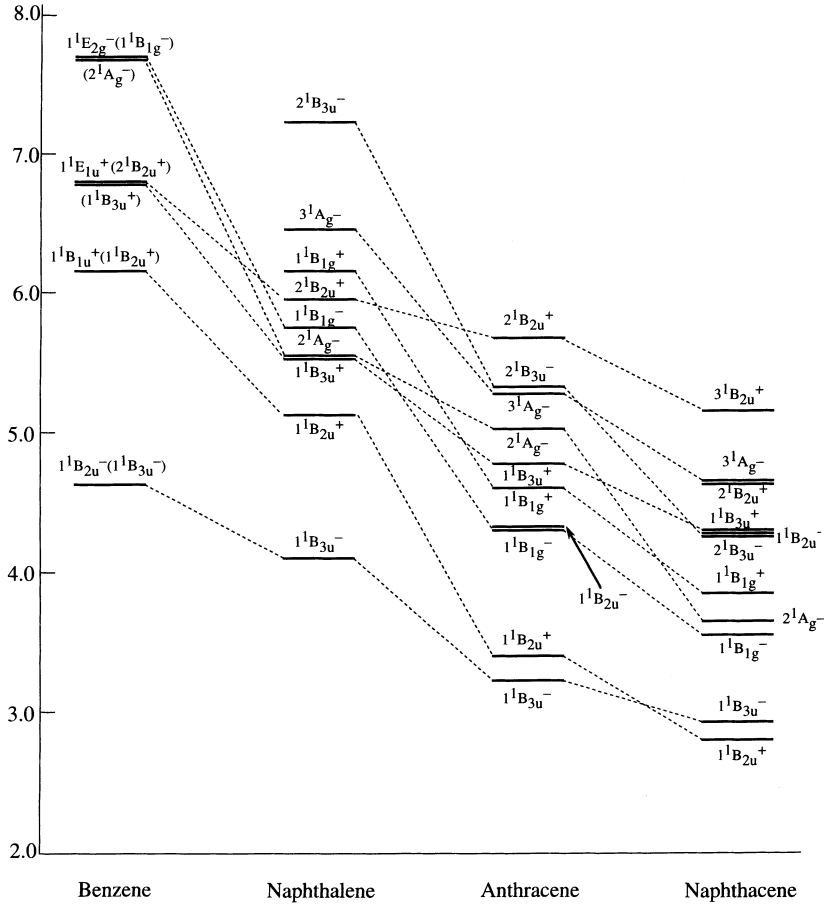

Fig. 2. MRMP excitation energies (eV) of the singlet excited states of polyacenes

wavefunction is dominated by the singly excited configuration of $1 \rightarrow 1'$. MRMP predicts that the excitation energy from $1^1A_g^-$ to $1^3B_{2u}^-$ is 1.51 eV. The singlet-triplet energy gap was observed to be in the range 1.25–1.30 eV by various experiments [43–45]. The difference between experiment and theory is about 0.2 eV.

The first triplet state above $1^3B_{2u}^-$ is the covalent $1^3B_{1g}^-$ state. The calculated T-T excitation energy and oscillator strength are 0.92 eV and 0.0002, respectively. This state is dominated by the singly excited configurations of $3 \rightarrow 1'$ and its conjugate. The absorption spectrum of naphthacene in alcohol solution shows this state occurs

at 1.29 eV [16]. Pariser [1] predicts 0.76 eV, which is much lower than the experimental value. Other calculations estimate the T-T excitation energy close to the experimental value.

The two single excitations of $1 \rightarrow 2'$ and $2 \rightarrow 1'$ result in a pair of covalent $^3B_{3u}^-$ and ionic $^3B_{3u}^+$ states. MRMP predicts that the $^3B_{3u}^-$ and $^3B_{3u}^+$ states lie at 1.45 and 2.01 eV above the lowest $1^3B_{2u}^-$ state. Theory predicts the existence of another u state between these two states. The second $2^3B_{2u}^-$ state mainly comes from transitions of $4 \rightarrow 1'$ and $1 \rightarrow 4'$ and the T-T excitation energy is calculated to be 1.76 eV.

The most intense triplet state is $1^3B_{1g}^+$. It is observed in the range 2.55–2.69 eV [16, 37, 46]. MRMP computes $1^3B_{1g}^+$ to appear at 2.51 eV with an oscillator strength of 0.4089. This state is described by a mixture of singly and doubly excited configurations of $3 \rightarrow 1'$, $2,1 \rightarrow (1')^2$ and their conjugates.

The one-electron excitation from the next HOMO to the next LUMO gives the $3^3B_{2u}^-$ state. MRMP places the state at 2.66 eV above $1^3B_{2u}^-$.

One-electron transitions of $1 \rightarrow 5'$ and $2 \rightarrow 3'$ and their conjugates result in a pair of covalent $1^3A_g^-$ and ionic $1^3A_g^+$ states. Contrary to the corresponding singlet states, the triplet $^3A_g^-$ and $^3A_g^+$ states are dominated by singly excited configurations. The minus state is predicted to appear at 2.93 eV and the plus state at 3.26 eV above the lowest triplet state. In addition, MRMP predicted another $^3A_g^-$ state exists above $1^3A_g^+$. The second $2^3A_g^-$ is computed to appear at 4.34 eV. This state is a mixture of the singly and doubly excited configurations. The computed oscillator strengths of these three transitions are 0.001, 0.007 and 0.002 from the lowest up. The intensity of the pseudoparity allowed transition to $1^3A_g^+$ is computed to be very weak since the $1^3A_g^+$ and the lowest $1^3B_{2u}^-$ states are mainly dominated by the $2 \rightarrow 3'$ and $1 \rightarrow 1'$ transitions, respectively. It is suggested that the band at 3.01 eV in the T-T absorption spectrum in tetrahydro-2-methylfuran solution is due to the $^3B_{2u}^- \rightarrow {}^3A_g^-$ transition [46]. The same peak is also found at 2.58 eV in the T-T absorption spectrum in alcohol solution [16] and at 2.60 eV in dilute solution [37]. In addition, two peaks are observed at 3.66 eV [16] and at 4.34 eV [37,46] in the T-T absorption spectrum. MRMP assigns the band observed at 3.01(2.58, 2.60) eV to the $^3B_{2u}^- \rightarrow {}^3A_g^-$ transition and the bands at 3.66 eV and 4.34 eV to the $^3B_{2u}^- \rightarrow 1^3A_g^+$ and $^3B_{2u}^- \rightarrow 2^3A_g^-$ transitions, respectively.

3.3 Low-lying $\pi \rightarrow \pi^*$ excited states of polyacenes

We now discuss the excited states of the polyacene family, from benzene to naphthacene. Figures 2 and 3

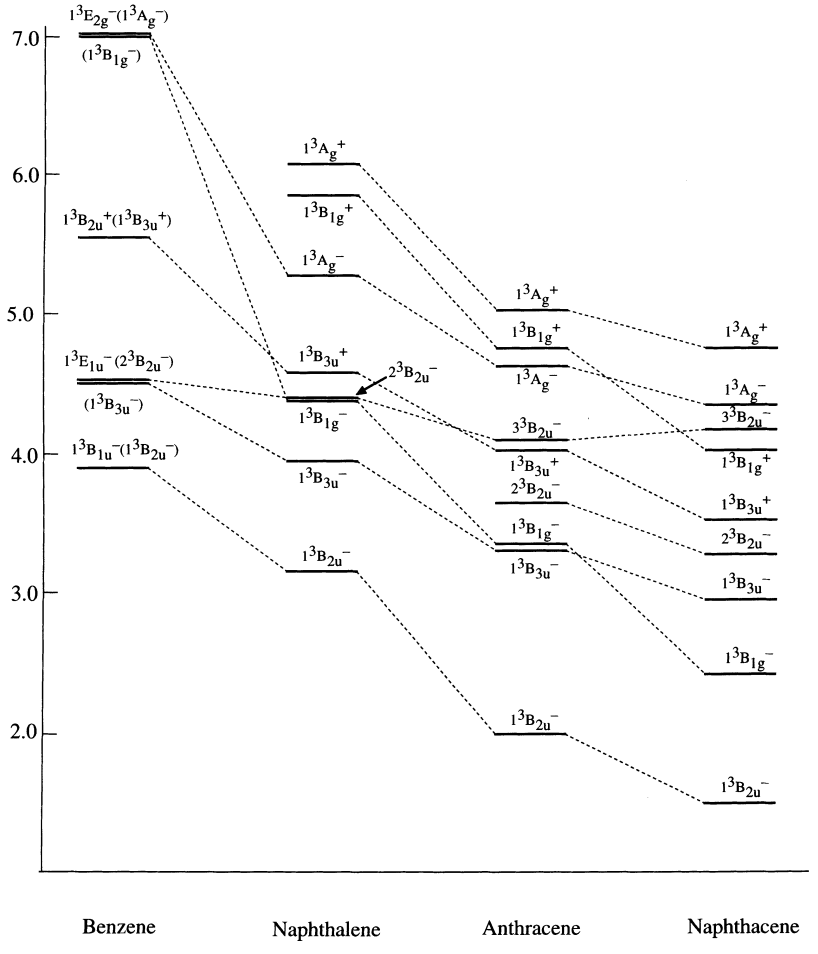

Fig. 3. MRMP excitation energies (eV) of the triplet excited states of polyacenes

present the interrelations between the low-lying $\pi \rightarrow \pi^*$ singlet and triplet excited states calculated with MRMP. Table 11 collects the MRMP results for the low-lying excited states from benzene to naphthacene. The energy levels of the lowest B_{3u}, B_{1g}, B_{2u}, and A_g states relative to the ground state of each polyacene are given separately in Figs. 4–7.

Table 11. MRMP excitation energies (eV) of polyacenes[a]

State	Benzene	Naphthalene	Anthracene	Naphthacene
Singlet states				
$1^1B_{3u}^-$	4.70	4.09	3.23	2.92
	(0.0000)	(0.0002)	(0.0004)	(0.0021)
$1^1B_{2u}^+$	6.21	4.62	3.40	2.80
	(0.0000)	(0.0616)	(0.0827)	(0.1039)
$1^1B_{3u}^+$	6.93	5.62	4.77	4.32
	(0.8912)	(1.3256)	(1.9377)	(2.3567)
$2^1B_{2u}^+$	6.93	5.95	5.67	5.16
	(0.8912)	(0.2678)	(0.1436)	(0.0002)
$1^1B_{1g}^-$	7.82	5.74	4.30	3.55
$2^1A_g^-$	7.82	5.65	5.03	3.66
Triplet states				
$1^3B_{2u}^-$	3.89	3.15	2.00	1.51
$1^3B_{3u}^-$	4.85	3.95	3.30	2.96
$2^3B_{2u}^-$	4.85	4.40	4.10	4.17
$1^3B_{3u}^+$	6.77	4.58	4.02	3.52
$1^3B_{1g}^-$	7.16	4.37	3.35	2.43
		(5×10^{-5})	(0.0003)	(0.0002)
$1^3A_g^-$	7.16	5.27	4.62	4.44
		(3×10^{-5})	(0.0012)	(0.0014)

[a] The oscillator strengths are given in parentheses

The two single excitations of $1 \rightarrow 2'$ and $2 \rightarrow 1'$ result in a pair of covalent $^1B_{3u}^-$ and ionic $^1B_{3u}^+$ states. Both states move to the red slowly with increasing number of rings and the interval between covalent and ionic states is almost constant. A similar trend is found between triplet $^3B_{3u}^-$ and $^3B_{3u}^+$ states. Moreover, the motion of triplet $^3B_{3u}$ states roughly parallels that of the singlet $^1B_{3u}$ states. That is, four B_{3u} states (singlet or triplet and covalent or ionic states) show a similar n dependence (n is the number of aromatic rings in the polyacenes). This is rather surprising since these excited states are quite different in nature. From the calculated data we see the following relation

$$E(^1B_{3u}^-) \approx E(^3B_{3u}^-) < E(^3B_{3u}^+) < E(^1B_{3u}^+)$$

It must be noted in Fig. 4 that the singlet and triplet *minus* states, $^1B_{3u}^-$ and $^3B_{3u}^-$, seem to converge to the same energy level with increasing number of rings.

A similar n dependence is also found in the B_{1g} states shown in Fig. 5. The four B_{1g} states move to the red the fastest with increasing number of rings. Both the $^1B_{1g}^-$ and $^3B_{1g}^+$ states come mainly from the single excitations of $1 \rightarrow 3'$ and $3 \rightarrow 1'$ but include a large fraction of doubly excited configurations of $(HOMO)^2 \rightarrow (LUMO)(LUMO+1)$ and its conjugate. The interval between covalent $^1B_{1g}^-$ and ionic $^1B_{1g}^+$ states, however,

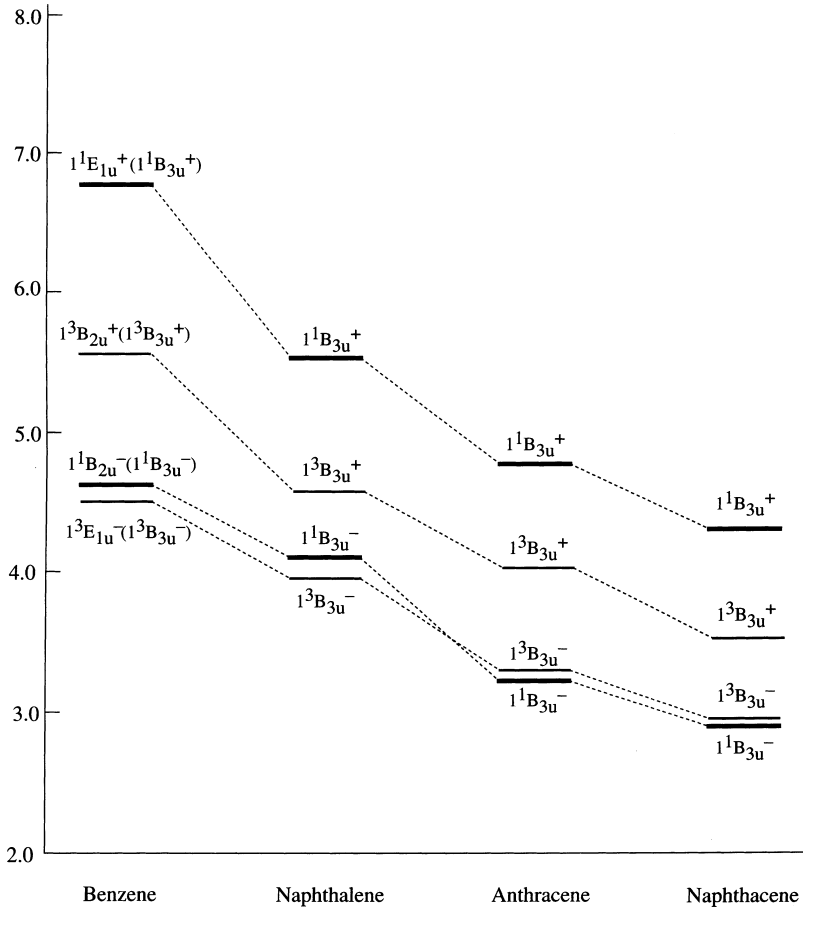

Fig. 4. MRMP energy levels (eV) of the polyacene $1^1B_{3u}^-$, $1^1B_{3u}^+$, $1^3B_{3u}^-$ and $1^3B_{3u}^+$ states relative to the ground state

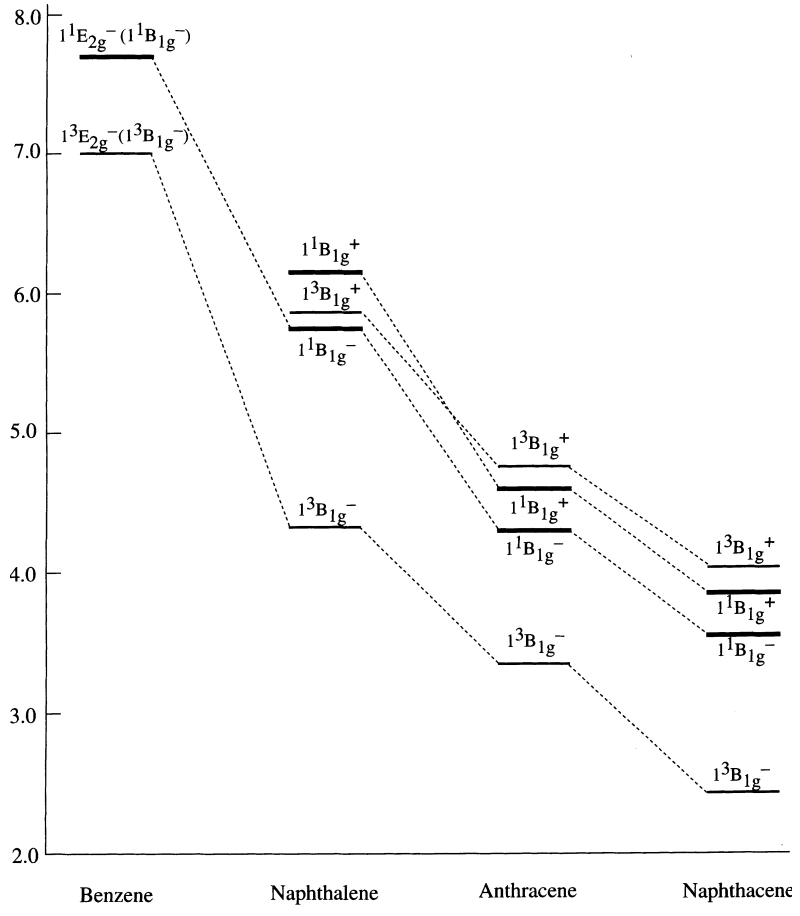

Fig. 5. MRMP energy levels (eV) of the polyacene $1^1B_{1g}^-$, $1^1B_{1g}^+$, $1^3B_{1g}^-$ and $1^3B_{1g}^+$ states relative to the ground state

remains roughly constant. Two triplet states also show a similar slope of the n dependence.

The covalent $^1B_{3u}^-$ state appears very weakly in the polyacenes since the transition $^1A_g \rightarrow {}^1B_{3u}^-$ is pseudoparity forbidden. On the other hand, the experimental oscillator strengths for the strongest long-axis polarized $1^1B_{3u}^+$ transitions display a peculiar pattern along the linear polyacene series. From benzene to anthracene the strength of this transition increases monotonically, while from anthracene to pentacene the strength remains essentially constant allowing for experimental uncertainties. This behavior was difficult to reproduce theoretically. All previous semiempirical calculations show that the $^1B_{3u}^+$ oscillator strength increases very rapidly throughout the series. In our calculations, agreement with experimental values is remarkably improved not only for the $^1B_{3u}^+$ transition but for all the observed transitions. For benzene to naphthacene, the calculated (experimental) $^1B_{3u}^+$ oscillator strengths are 0.891 (1.25, 0.88), 1.326 (1.21, 1.3, 1.70), 1.938 (2.28), and 2.357 (1.75), respectively. However, the transition still shows the same monotonic increase along the series.

The $1 \rightarrow 1'$ excitation gives rise to the first ionic $1^1B_{2u}^+$ state while the $2 \rightarrow 2'$ transition gives rise to the second (third in naphthacene) ionic $2^1B_{2u}^+$ state. As can be seen in Fig. 6 the $1^1B_{2u}^+$ state moves the fastest to the red with increasing rings while the $2^1B_{2u}^+$ state moves the most slowly. The interval between the two states increases with increasing n. The slope of the n dependence of $1^1B_{2u}^+$ is much steeper than that of $1^1B_{3u}^-$. Thus, the crossover between $1^1B_{3u}^-$ and $1^1B_{2u}^+$ occurs at around anthracene. With the present scheme the well-known inversion between the p and α bands occurs going from anthracene to naphthacene, while with Pariser's SCI it occurs between naphthalene and anthracene.

The short-axis polarized $1^1B_{2u}^+$ band increases in intensity with increasing n since the $1 \rightarrow 1'$ transition becomes dominant with increasing n. On the other hand, the $2^1B_{2u}^+$ band originating from $2 \rightarrow 2'$ decreases in intensity with the increase in the number of rings due to the considerable admixture of the $3 \rightarrow 3'$ transition with an antiparallel transition moment vector.

Triplet $1 \rightarrow 1'$ and $2 \rightarrow 2'$ transitions yield excited $^3B_{2u}^-$ states with covalent character. The $1^3B_{2u}^-$ state is the lowest triplet excited state in each polyacene. The n dependence of the triplet $^3B_{2u}^-$ states is less steep compared to that of the corresponding singlet $^1B_{2u}^+$ states.

As shown by Coulson [47], all polyacenes have specific orbitals with the characteristic values of $\lambda = \pm 1$ the in Huckel approximation. The $^1B_{2u}^+$ and $^3B_{2u}^-$ states originate from the single excitation from the occupied orbital with $\lambda = 1$ to the conjugated unoccupied orbital with $\lambda = -1$. Thus, they have the same excitation energy for all the polyacenes in the Hückel approximation. The excitation energies of this type are expected to remain roughly constant. The singlet $2^1B_{2u}^+$ excitation energies computed with MRMP are 6.93 eV (benzene), 5.95 eV

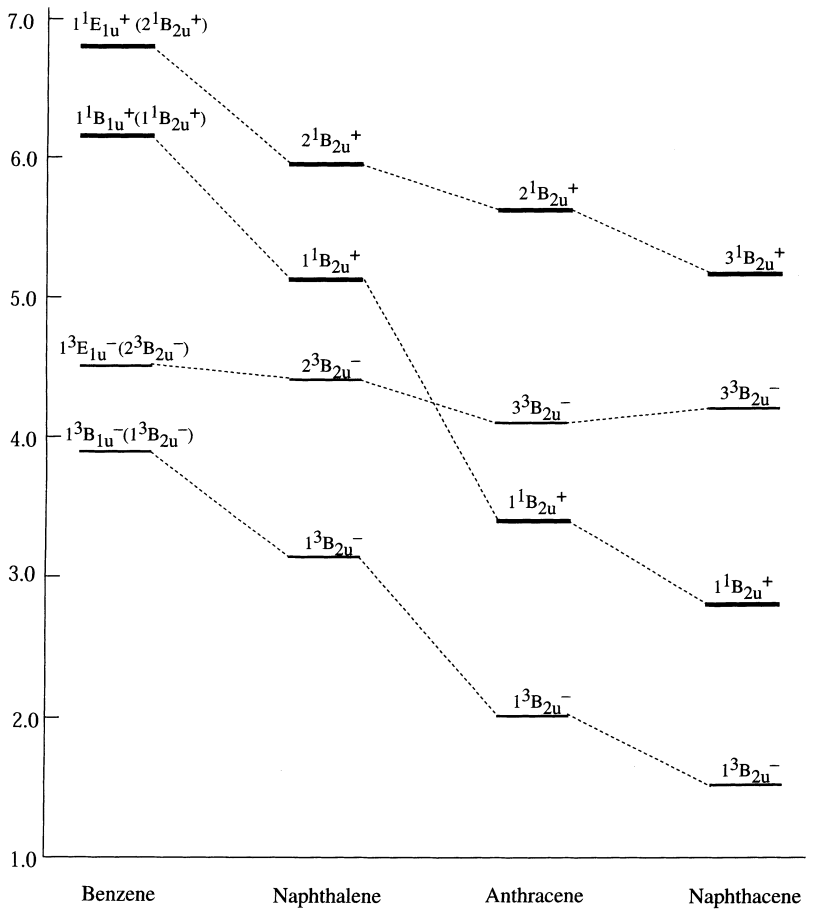

Fig. 6. MRMP energy levels (eV) of the polyacene $1^1B_{2u}^+$, $2^1B_{2u}^+$, $1^3B_{2u}^-$ and $2^3B_{2u}^-$ states relative to the ground state

(naphthalene), 5.67 eV (anthracene) and 5.16 eV (naphthacene) and those for triplet $2^3B_{2u}^-$ excitation are 4.53 eV (benzene), 4.40 eV (naphthalene), 4.10 eV (anthracene), and 4.17 eV (naphthacene). Thus, the triplet $2^3B_{2u}^-$ state moves to the red the most slowly.

The fourth excited state of benzene, $^1E_{2g}^-$, is a doubly excited state and the wavefunction is represented by the three Dewar structures in a CAS valence bond description [8]. The degenerate $^1E_{2g}$ states split into 1^1B_{1g} and 2^1A_g in larger polyacenes. The strong energy depression of $1^1B_{2g}^-$ and $2^1A_g^-$ in going from benzene to naphthacene is due to an admixture of low energy double excitations. With increasing number of aromatic rings the double excitation becomes predominant. The $2^1A_g^-$ state as well as the $1^1B_{1g}^-$ state approach the first excited state with increasing number of rings. However, the slope of the n dependence of $2^1A_g^-$ and $1^1B_{1g}^-$ is similar to that of $1^1B_{2u}^+$ in going from naphthalene to naphthacene. Thus, contrary to the polyene case, the crossover between $2^1A_g^-$ and $1^1B_{2u}^+$ does not seem to occur in polyacenes.

The triplet $^3A_g^-$ state is a singly excited state and the n dependence is much less steep compared to that of the singlet $2^1A_g^-$. The interval between singlet and triplet $^1A_g^-$ states decreases with increasing number of rings and the doubly excited singlet $2^1A_g^-$ state is 0.78 eV lower than the corresponding triplet $1^3A_g^-$ state in naphthacene. This is true for the doubly excited $1B_{1g}^+$ state. The $1^1B_{1g}^+$ state is lower than the $1^3B_{1g}^+$ state after naphthalene.

4 Summary

Multireference perturbation theory with CASSCF reference functions is applied to the study of the valence $\pi \rightarrow \pi^*$ excited states of anthracene and naphthacene. MRMP satisfactorily describes the ordering of low-lying valence $\pi \rightarrow \pi^*$ excited states. The calculated transition energies are in good agreement with experimental data although comparison with experiment is not straightforward. MRMP predicts the valence excitation energies with an accuracy of 0.15 eV for anthracene and 0.25 eV for naphthacene.

The covalent minus states always give lower energies than the corresponding ionic plus states. The ionic plus states are dominated by single excitations but covalent minus states (especially g states) include a large fraction of doubly excited configurations. For singlet spin states, a double excitation of $(\text{HOMO})^2 \rightarrow (\text{LUMO})^2$ strongly admixes to the wavefunctions of the $2^1A_{1g}^-$ state. Also the doubly excited configuration of $(\text{HOMO})^2 \rightarrow (\text{LUMO})(\text{LUMO}+1)$ and its conjugate make a significant contribution to $1^1B_{1g}^-$ of polyacenes. Most low-lying triplet states are dominated by singly excited configurations except $1^3B_{1g}^+$, which is a mixture of single and double excitations.

The excited states of anthracene and naphthacene are compared with those of previously studied benzene and naphthalene. The present calculation predicts that going from anthracene to naphthacene there is a symmetry

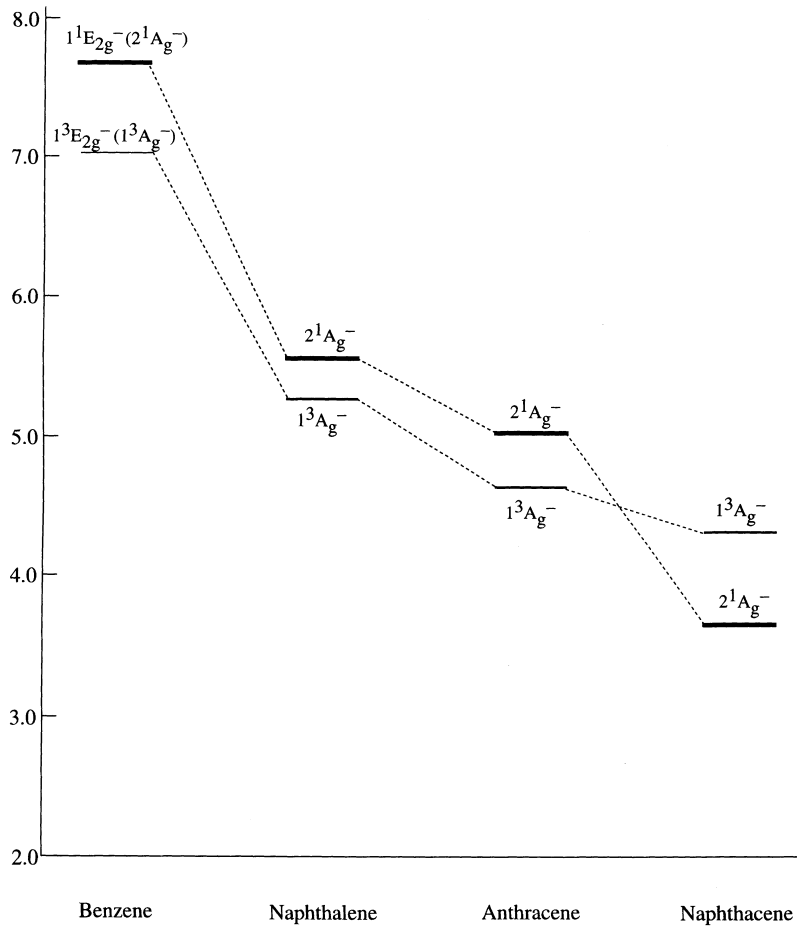

Fig. 7. MRMP energy levels (eV) of the polyacene $2^1A_g^-$ and $1^3A_g^-$ states relative to the ground state

reversal of the two lowest singlet state transitions, but not for the triplet, just as indicated by the experimental data. Some general trends of polyacene excited states with the increase in the number of rings are also derived from the MRMP results for benzene to naphthacene.

It is hoped that the results described in this paper are to some extent transferable and thus provide a reasonable basis for a description of the excited states of larger polyacenes.

Acknowledgements. This work has been supported in part by a grant-in-aid for Scientific Research from the Ministry of Education, Science and Culture and the AGS project. We are also grateful to the Genesis Research Institute Inc. for financial support for this research. The computations were carried out on an IBM SP2 at the Intelligent Modeling Laboratory (IML) of the University of Tokyo. The CASSCF reference wavefunctions were obtained using the MOLPRO [48] program. The perturbation calculations were performed with the MR2D program [49].

References

1. Pariser R (1956) J Chem Phys 24: 250
2. (a) Andersson K, Malmqvist P, Roos BO, Sadlej AJ, Wolinski K (1990) J Phys Chem 94: 5483; (b) Andersson K, Malmqvist P, Roos BO (1992) J Chem Phys 96: 1218
3. (a) Hirao K (1992) Chem Phys Lett 190; 374; (b) Hirao K (1992) Chem Phys Lett 196: 397; (c) Hirao K (1993) Chem Phys Lett 201: 59; (d) Hirao K (1992) Int J Quantum Chem Symp 26: 517
4. Nakayama K, Nakano H, Hirao K (1998) Int J Quantum Chem 66: 157
5. (a) Hirao K, Nakano H, Hashimoto T (1995) Chem Phys Lett 235: 430; (b) Hashimoto T, Nakano H, Hirao K (1996) J Chem Phys 104: 6244; (c) Hashimoto T, Nakano H, Hirao K (1998) Theochem (Huzinaga Special Issue) (in press)
6. (a) Pariser R, Parr RG (1953) J Chem Phys 21: 466, 767; (b) Pople JA (1953) Trans Faraday Soc 49: 1375
7. (a) Coulson CA, Rushbrooke GS (1940) Proc Camb Phil Soc 36: 193; (b) Koutecky J (1966) J Chem Phys 44: 3702; (c) Cizek J, Paldus J, Hubac I (1974) Int J Quantum Chem 8: 951
8. (a) Hirao K, Nakano H, Nakayama K, Dupuis M (1996) J Chem Phys 105: 9227; (b) Hirao K, Nakano H, Nakayama K (1997) J Chem Phys 107: 9966
9. (a) Siegbahn PE, Heiberg A, Roos BO, Levy B (1980) Phy Scr 21: 323; (b) Roos BO, Taylor PR, Siegbahn PE (1980) Chem Phys 48: 157; (c) Roos BO (1980) Int J Quantum Chem Symp 14: 175
10. (a) Hudson BS, Kohler BE (1972) Chem Phys Lett 14:299; (b) Hudson BS, Kohler BE, Schulten K (1982) In: Excited states 6:1. Academic Press, New York
11. In Clar's notation these are the α, p and β bands which correspond to the polyacenes $^1B_{3u}^-$, $^1B_{2u}^+$, and $^1B_{3u}^+$ states, respectively; Clar E (1964) In: Polycyclic hydrocarbons. Springer, Berlin Heidelberg New York
12. In Platt's notation these are the ^1L_b, ^1L_a, and ^1B_b states which correspond to the polyacene $^1B_{3u}^-$, $^1B_{2u}^+$, and $^1B_{3u}^+$ states, respectively; Klevens HB, Platt JR (1949) J Chem Phys 17: 470
13. Dunning TH (1989) J Chem Phys 90: 1007
14. Cruickshank DWJ (1956) Acta Crystallog 9: 915
15. Campbell RB, Robertson JM (1962) Acta Crystallog 15: 289
16. Meyer YH, Astier R, Leclercq JM (1972) J Chem Phys 56: 801

17. Tavan O, Schulten K (1979) J Chem Phys 79: 5414
18. Baldo M, Grassi A, Pucci R, Tomasello (1982) J Chem Phys 77: 2438
19. Ramasesha S, Galvao DS, Soos ZG (1993) J Phys Chem 97: 2823
20. Alderich DM, Mathies R, Albrecht AC (1974) J Mol Spectrosc 51: 166
21. Lipari NO, Duke CB (1975) J Chem Phys 63: 1768
22. Wolf J, Hohlneicher G (1994) Chem Phys 181: 185
23. Platt JR (1949) J Chem Phys 17: 484
24. Clar E (1950) Spectrochim Acta 4: 116
25. Mason SF, Peacock RD (1973) Chem Phys Lett 21: 406
26. Inoue H, Hoshi T, Masamoto T, Shiraishi J, Tanizaki Y (1971) Ber Bunsenges Phys Chem 75: 441
27. Sackmann E, Mohwald H (1973) J Chem Phys 58: 5407
28. Bergman A, Jortner J (1972) Chem Phys Lett 15: 309
29. Steiner RP, Michl J (1978) J Am Chem Soc 100: 6861
30. Lambert WR, Felker PM, Syage JA, Zewail AH (1984) J Chem Phys 81: 2195
31. Dick B, Hohlneicher G (1981) Chem Phys Lett 83: 615
32. Margulies L, Yogev A (1978) Chem Phys 27: 89
33. Suzuki H (1967) Electronic absorption spectra and geometry of organic molecules. Academic Press, New York
34. Michl J, Thulstrup EW, Eggers JH (1974) Ber Bunsenges Phys Chem 78: 575
35. Lyons LE, Morris GC (1960) J Mol Spectrosc 4: 480
36. Schiedt J, Weinkauf R (1997) Chem Phys Lett 266: 201
37. Porter G, Windsor MW (1958) Proc Roy Soc London Ser A 245: 235
38. Nickel B, Roden G (1977) Ber Bunsenges Phys Chem 81: 281
39. Zimmermann H, Joop N (1960) Ber Bunsenges Phys Chem 64: 1215
40. Berlman IB (1971) Handbook of flourescence spectra of aromatic molecules, 2nd edn. Academic Press, New York
41. Bree A, Lyons LE (1960) J Chem Soc 5206
42. Canuto S, Zerner MC, Diercksen GHF (1991) Astrophys J 377: 150
43. Tomkiewicz Y, Groff RP, Avakian P (1971) J Chem Phys 54: 4504
44. Sabbatini N, Indelli MT, Gandolfi MT, Balzani V (1982) J Phys Chem 86: 3585
45. McGlynn SP, Azumi T, Kasha M (1964) J Chem Phys 51: 507
46. Pavlopoulos TG (1972) J Chem Phys 56: 227
47. Coulson CA (1948) Proc Phys Soc London Ser A 60: 257
48. MOLPRO is a package of ab initio programs written by Werner HJ, Knowles PJ, with contributions from Almlof J, Amos RD, Deegan MJO, Elbert ST, Hampel C, Meyer W, Peterson K, Pitzer R, Stone AJ, Taylor PR, Lindh R
49. (a) Nakano H (1993) J Chem Phys 99: 7983; (b) Nakano H (1995) MR2D Version 2. University of Tokyo